BMC Medical Imaging

RESEARCH

Open Access

# Development of optimised protocols for paediatric whole-body computed tomography examinations: a figure-of-merit approach

Jacob Leonard Ago[1,2*], Stephen Inkoom[3,4], Benard Ohene-Botwe[5], Alise Larsen[6] and Ingerd Skaaret Berg[6]

## Abstract

**Background** Whole-body computed tomography (WBCT) technique involves higher radiation doses, resulting in increased stochastic health risks, especially when used for paediatric patients. Hence, protocol optimisation is recommended to maximise its benefit-risk ratio, with several available strategies to achieve it. This study used the figure-of-merit (FOM) approach to develop optimised protocols for paediatric WBCT examinations. The rationale is to enhance diagnostic accuracy while minimising radiation exposure, ultimately improving patient safety and outcomes for paediatric patients undergoing WBCT.

**Methods** Newborn and child (5-year-old) anthropomorphic phantoms were scanned with different scan protocols and evaluated for dose and image quality using the CT-Expo and ImageJ programs, respectively. The protocols for trunk examinations were divided into arterialphase-only and combined arterial and venous phase to develop appropriate protocols based on patients' initial focused assessment with sonography for trauma (FAST) results. The protocols with the highest FOMs were selected as the best optimised protocols.

**Results** The estimated WBCT ED ($WB_{ED}$) for the optimised protocols ranged from 2.6 mSv to 5.8 mSv with estimated FOM of 3.83 to 59.35. The mean effective doses (EDs) for newborn and child arterial phase-only protocols were not significantly lower than the combined arterial and venous phase protocols ($p = 0.069$, 0.082 respectively), while the mean signal-to-noise ratio of the combined phase protocols for newborn and child phantoms were insignificantly higher than the single-phase protocol ($p = 0.089$, 0.662 respectively).

**Conclusion** The estimated $ED_{WB}$ from this study were lower than established values. The selected protocols are recommended for newborns and children (1–7 years) using the GE Revolution CT and Siemens SOMATOM Definition Edge CT scanners.

**Keywords** Whole body computed tomography, Figure of merit, Anthropomorphic Phantom, Paediatric, Dose optimisation

*Correspondence:
Jacob Leonard Ago
jacobleonardago@gmail.com

Full list of author information is available at the end of the article

## Introduction

Computed tomography (CT) is regarded as a high radiation dose modality with associated higher dose levels than other imaging modalities such as general X-ray examinations [1, 2]. Among the numerous advantages of CT is its ability to assess multi-trauma patients with injuries to multiple body parts using a whole-body CT (WBCT) technique [3–7]. There is an increased use of WBCT in trauma centres due to its efficient diagnosis [5]. Nonetheless, this technique involves even higher radiation doses [4, 8, 9]. Notably, Jiang and Wang [9] reported that depending on the scanner and the protocols used, the effective dose (ED) from a single WBCT examination could be as high as 30 mSv.

To reduce the risk of stochastic health associated with WBCT, it is vitally important for practitioners to follow radiation protection guidelines and recommendations [10]. One of the recommendations to maximise the benefit-risk ratio during medical imaging in general and WBCT in particular is to optimise examination protocols [11, 12].

Strategies for optimising CT radiation dose include scan length optimisation, adjustment of exposure parameters, and proper patient positioning [13–15]. Pace and Borg [16] contend that a combination of dose and image quality metrics into a figure-of-merit (FOM) enables the comparison of image quality metrics independently of dose, an approach that ensures a balance between dose and image quality. The FOM is a single-value descriptor of performance, with desirable attributes in the numerator (image quality metric) and undesirable attributes in the denominator (dose metric).

Many studies on protocol optimisation have focused on adults and/or general paediatric CT. Subsequently, facilities without age-specific paediatric protocols may use modified adult CT protocols, resulting in increased risk of stochastic health effects [17]. This study aims to develop optimised protocols for paediatric WBCT examinations using the FOM approach.

## Materials and methods

### Study design and study site

A phantom-based experimental study design [18] was adopted to develop optimised protocols for paediatric WBCT examinations at the Department of Radiology, Innlandet Hospital Trust, Hamar, Norway.

### Materials

The CT examinations were performed with the General Electric (GE) Revolution™ CT (GE Medical Systems, Waukesha, United States of America) and the Siemens SOMATOM Definition Edge CT scanners (Siemens Healthineers, Erlangen, Germany). Scans were performed on Kyoto Kagaku newborn (PBU-80, ≤ 1-year old) and child (PBU-70, 5-year-old) anthropomorphic phantoms (Kyotokagaku America Inc., Los Angeles, United States of America) positioned on CM Trauma-Mattress™ (Comfort Medical AB, Sweden). In addition, quality control (QC) tests were performed with Black Piranha 657 (B2-16020228, RTI, Sweden) and Catphan® 500 (The phantom laboratory, Salem, NY, USA).

### Methods

#### *Quality control checks*

QC checks on both scanners were performed prior to the study in line with the International Electrotechnical Commission's (IEC) standards [19]. The tests included dose measurement free in air, CT number, homogeneity, and noise.

#### *CT examinations*

The two phantoms were positioned on an intra-hospital trauma mattress (Fig. 1) and scanned in turns with different protocols for both CT scanners. The Deep Learning Image Reconstruction (DLIR) 'high' strength level and the Advanced Modeled Iterative Reconstruction (ADMIRE) strength 3 were used for examinations with the GE and Siemens scanners respectively. Head examinations were performed with non-contrast head protocols while the body examinations were performed with either arterial phase chest-abdomen-pelvis (CAP) or arterial phase CAP and venous phase abdomen-pelvis (AP) examination. The height of the table was maintained at isocenter for all examinations to avoid possible displacement. The images obtained from the GE and Siemens scanners had slice thickness of 0.625 mm and 0.750 mm respectively. The average scan length, pitch, and slice thickness used for each scanner have been provided in Table 1.

#### *Effective dose and organ dose*

The CT-Expo software version 2.5 (SASCRAD, Fritz-Reuter-Weg, Buchholz, Germany) was used to estimate the ED and organ dose for all tested protocols and the organ doses associated with the optimised protocols. The BABY and CHILD models in CT-Expo were used for the baby and child phantom examinations respectively. Additionally, tissue weighting factors prescribed in ICRP publication 103 were adopted for this study. Table 2 shows the various scan lengths used to estimate the ED and organ dose from CT-Expo.

#### *Image quality (IQ) assessment*

IQ assessment was undertaken by qualitative scoring and quantitative measurements. Qualitatively, two independent radiologists ranked the images on a 5-point Likert scale [10] for artefacts, image noise, contrast, organ visibility, and overall diagnosability. Inter-rater agreement between the two radiologists was assessed with

**Fig. 1** Child phantom positioned on the trauma mattress

**Table 1** Average CT scan parameters

| Parameter | Newborn phantom | | Child phantom | |
|---|---|---|---|---|
| | GE scanner | Siemens scanner | GE scanner | Siemens scanner |
| Scan length [cm] | 22.81 | 22.59 | 44.46 | 45.82 |
| Pitch | 0.88 | 1.40 | 0.68 | 1.33 |
| Slice thickness [mm] | 0.63 | 0.75 | 0.63 | 0.75 |

the Cohen's kappa coefficient. In contrast, quantitative measurements were performed with the ImageJ software version 1.54c (Wayne Rasband and Contributors, National Institutes of Health, USA). The SNR was used as the image quality descriptor and computed according to Eq. 1, given by Gariani et al. [10].

$$SNR = \frac{Mean\ Signal\ in\ ROI}{Standard\ Deviation\ in\ ROI} \quad (1)$$

In determining the signal and noise for body examinations, three circular regions of interest (ROIs) of equal dimensions (5.0 mm x 5.0 mm) were drawn on three different images of the liver (for the child phantom) and heart (for the newborn phantom) at the same slice position. For the head examinations, four square ROIs of equal dimensions (5.0 mm x 5.0 mm) were drawn on the most homogenous axial images. Figure 2 shows how the signal and standard deviations (noise) were obtained from the ImageJ software version 1.54c (Wayne Rasband and Contributors, National Institutes of Health, USA).

### *Selection of optimum protocols*

The best optimum protocols were selected using the FOM, determined as the ratio of the square of the SNR to the ED (Eq. 2).

$$FOM = \frac{SNR^2}{ED} \quad (2)$$

According to Pace and Borg [16], the FOM value increases with an increase in efficacy. A higher FOM,

**Table 2** Scan lengths used in dose calculation from CT-Expo

| | Scan range | | | | Scan length | |
|---|---|---|---|---|---|---|
| | From z- | | To z+ | | L (cm) | |
| | Male | Female | Male | Female | Male | Female |
| Newborn Phantom | | | | | | |
| Head | 28 | 28 | 38 | 38 | 10 | 10 |
| Chest | 14 | 11 | 25 | 22 | 11 | 11 |
| Abdomen-Pelvis | 0 | 1 | 18 | 18 | 18 | 18 |
| CAP | 1 | 1 | 23 | 22 | 22 | 21 |
| Child Phantom | | | | | | |
| Head | 48 | 48 | 63 | 63 | 15 | 15 |
| Chest | 26 | 24 | 43 | 40 | 17 | 16 |
| Abdomen-Pelvis | 0 | 1 | 28 | 27 | 28 | 26 |
| CAP | 0 | 1 | 41 | 40 | 41 | 39 |

**Key**: z- = start of scan range; z+ = end of scan range; L = estimated scan length; CAP = chest-abdomen-pelvis

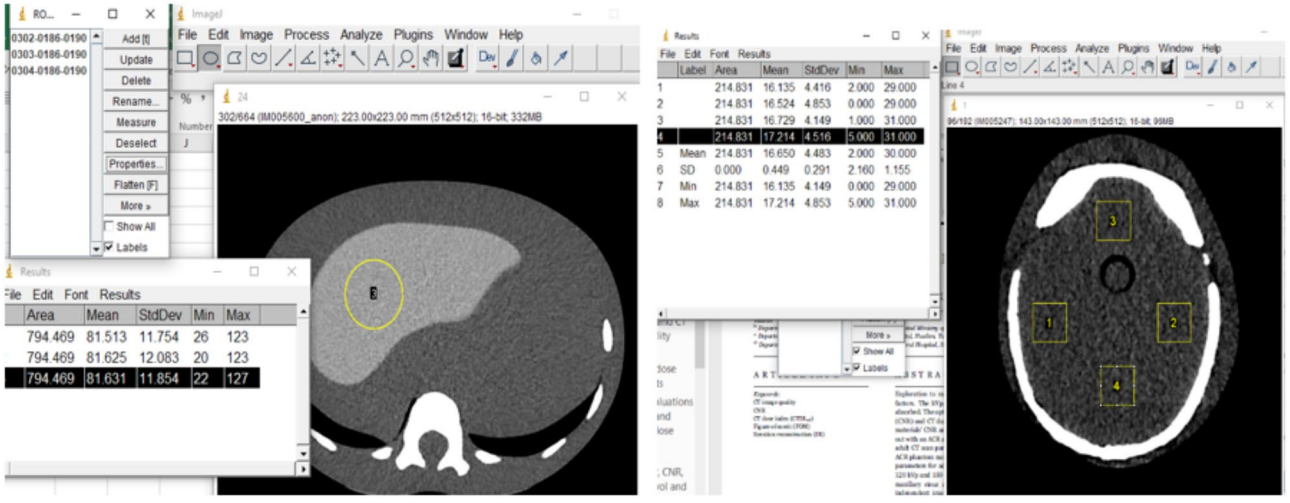


**Fig. 2** Signal and noise measurements in ImageJ software

therefore, indicates an increased efficiency of the studied protocol; hence, for each set of protocols, the protocol with the highest FOM was selected.

#### *Data analysis*

The IBM SPSS Statistics for Windows, Version 26.0 (IBM Corp., Armonk, N.Y., USA) was used to undertake both descriptive and inferential analysis of the data. Due to the non-normally distributed nature of the data from a Shapiro-Wilk test ($p = 0.001$), a Mann-Whitney U-test was used for inferential analysis and statistical differences were considered significant at $p < 0.05$.

## Results

### QC tests

Results for all tests performed were within the tolerance limits and are available on request.

### Effective dose and image quality

#### *Inter-observer reliability (IOR) for qualitative IQ assessment*

The IOR, assessed with Cohen's Kappa, ranged from 0.621 to 0.831 indicating a moderate to strong agreement between the two radiologists [20].

#### *Mean ED and IQ scores*

The average ED of newborn trunk examinations performed with only arterial phase protocol was 69.83% lower than the ED of newborn trunk examinations performed with both arterial and venous phase protocols, although not statistically significant (U = 11.00, $p = 0.069$). Similarly, even though the average ED of examinations performed with arterial phase CAP protocol for the child phantom was 23.53% lower than the ED examinations performed with arterial phase CAP + venous phase AP protocols, a non-significant difference (U = 5.00, $p = 0.082$) was observed.

For the IQ, there were no statistically significant differences ($p > 0.05$) in the mean IQ scores between the arterial phase CAP and the arterial phase CAP + venous phase AP protocols, although the tests revealed higher SNRs for the later while the former had higher qualitative IQ scores than the later for both newborn and child phantoms as presented in Table 3.

### Selection of optimised protocols

#### *GE scanner*

#### *Head protocols*

One examination each was performed with the newborn and child phantoms. Both protocols were selected as they were adjudged to be of good diagnostic quality.

**Newborn CAP protocols** Five arterial phase CAP protocols were tested for the newborn examinations, with Protocol GB1 producing the least ED and the highest FOM. For the same set, Protocol GB3 was scanned in two series, with the chest scanned separately from the AP. Protocol GB5 was a variant of Protocol GB1, with noise index (NI) = 20 and resulted in an ED of 1.60 mSv and SNR of 1.34. Even though Protocol GB4 had the highest SNR, the associated DLP and $CTDI_{vol}$ were 101.13% and 134.34% higher than Protocol GB1. Additionally, Protocol GB3 was scanned in two series, with the chest scanned separately from the AP. The overlap, due to the multiple sequence, resulted in an increased effective dose.

Protocol GB1 was subsequently selected as the best-optimised protocol due to its high FOM. In contrast, three newborn arterial phase CAP + venous phase AP protocols were tested. Protocol GBI had the least effective dose and highest SNR. Protocols GBII and GBIII had reduced pitch and resulted in increased EDs, although the former, with tube voltage of 100 kVp, resulted in higher ED than the latter with 80 kVp. Eventually, Protocol GBI was selected as the best optimised protocol.

**Table 3** Mean ED and IQ scores

| IQ Descriptor | Newborn [Mean ± Standard Deviation] | | *p*-value | Child [Mean ± Standard Deviation] | | *p*-value |
|---|---|---|---|---|---|---|
| | 9.1 A (*n* = 7) | 9.1B (*n* = 5) | | 9.1 A (*n* = 5) | 9.1B (*n* = 4) | |
| **Effective Dose** | | | | | | |
| ED (mSv) | 1.79 ± 0.78 | 3.04 ± 1.67 | 0.069 | 5.24 ± 2.32 | 6.49 ± 1.17 | 0.082 |
| **Quantitative IQ** | | | | | | |
| SNR | 1.76 ± 0.46 | 1.82 ± 0.91 | 0.894 | 5.24 ± 2.32 | 6.49 ± 1.17 | 0.662 |
| **Qualitative IQ** | | | | | | |
| Artifacts | 3.00 ± 0.63 | 2.80 ± 0.84 | 0.661 | 2.83 ± 0.82 | 2.70 ± 0.67 | 0.630 |
| Noise | 3.45 ± 0.69 | 3.20 ± 1.10 | 0.827 | 3.67 ± 0.52 | 3.20 ± 1.10 | 0.776 |
| Contrast | 3.45 ± 0.69 | 3.40 ± 0.89 | 1.00 | 3.60 ± 0.55 | 3.33 ± 0.52 | 0.776 |
| Organ Visibility | 3.09 ± 0.54 | 1.86 ± 0.55 | 0.221 | 3.67 ± 0.52 | 3.20 ± 0.84 | 0.630 |
| Overall Diagnosability | 3.27 ± 0.61 | 3.00 ± 0.79 | 0.459 | 3.67 ± 0.52 | 3.40 ± 0.96 | 0.570 |

**Key**: *SNR = signal-to-noise ratio; ED = effective dose from CT-Expo; 9.1 A = examinations performed with* arterial phase CAP only; 9.1B = examinations performed with arterial phase CAP + venous phase AP protocols

**Child CAP protocols** Three (3) arterial phase CAP protocols were tested with the child phantom. Protocol GC2 had the least ED whereas protocol GC3 had the highest ED. All the studied protocols had the same average overall subjective IQ score (IQ = 4 out of 5). Protocol GC4 was selected as the best-optimised protocol for its high FOM. In contrast, two arterial phase CAP + venous phase AP protocols were tested in this series. Protocol GCI with auto-prescription and NI = 26 had a higher effective dose than protocol GCII that was scanned without auto-prescription. However, protocol GCI was selected as the optimised protocol due to its higher SNR and FOM than protocol GCII and was also adjudged to have a better overall qualitative IQ.

Table 4 describes the newborn and child protocols for the GE scanner.

#### *Siemens scanner*

**Head protocols** One examination each was performed with the newborn and child phantoms. The two were accepted due to their adequate diagnostic ability.

**Newborn CAP protocols** In this series, two arterial phase CAP protocols were proposed and tested. Protocol SB1 produced a higher ED (1.60 mSv) and a lower FOM (9.17) than Protocol SB2 (ED = 1.50 mSv, FOM = 13.74). Additionally, Protocol SB2 had a better qualitative IQ score than Protocol SB1 and was selected as the better of the two protocols. Similarly, two arterial phase CAP + venous Phase AP protocols were tested. Protocol SBI was selected as the optimised protocol due to its better SNR, FOM and qualitative IQ score than Protocol SBII, although the ED associated with the former was 5.56% higher (Table 5).

**Child CAP protocols** Two arterial phase CAP protocols and two two arterial phase CAP + venous Phase AP protocols were tested. Protocol SC1 was scanned with a 12.5% higher tube voltage than Protocol SC2. The former protocol was selected as the optimised protocol for arterial phase CAP examinations due to its higher FOM. Similarly, Protocol SCII scanned with a 12.5% higher tube voltage resulted in a slightly better image quality than Protocol SCI (Table 5) and was subsequently selected for arterial phase CAP + venous Phase AP examinations.

#### Organ doses from the optimised protocols

Doses to the brain and eye lenses were estimated using CT-Expo. The brain received lower dose than the eye lenses for both newborn protocol (16.25 mSv vs. 18.70 mSv) and child phantom protocols (22.9 mSv vs. 29.05 mSv). Regarding the trunk examinations, the testis received the minimum dose of 1.05 and 2.10 mSv from newborn 9.1 A and 9.1B protocols respectively. The kidneys, bladder, prostate, ovaries, and uterus received the maximum dose of 2.45 mSv in the newborn 9.1 A protocols, whereas the ovaries and uterus received a maximum dose of 4.3 mSv in the newborn 9.1B protocols. For examinations performed with the child phantom, the oesophagus received a minimum dose of 4.05 mSv and 4.30 mSv from the 9.1 A and 9.1B protocols respectively. It was also found that the breast received a maximum dose of 4.95 mSv from the 9.1 A protocols while the kidneys received a maximum dose of 6.7 mSv from the 9.1B protocols. The organ doses associated with all examinations performed with the 9.1 A protocols had a median value of 3.25 mSv (95% *C.I* = 2.69 to 3.62 mSv). This was statistically significantly lower than the organ doses from all examinations performed with the 9.1B protocols, median = 4.15 mSv (95% *C.I* = 4.13 to 5.12 mSv) [U = 249.00, $p < 0.001$].

## Discussion

The study focussed on developing optimised age specific paediatric WBCT protocols using the FOM approach. The protocols were divided into examinations with only arterial phase CAP and arterial phase CAP + venous phase AP. This was necessary to obtain protocols that can adequately diagnose trauma conditions based on results from focused assessment with sonography for trauma (FAST), a diagnostic test used to evaluate intraperitoneal fluid in patients with suspected blunt trauma to the torso [21].

#### Effective dose

The double sequence (9.1B) protocols resulted in higher EDs than the single sequence (9.1 A) protocols for both phantoms, albeit there were no statistically significant differences (Table 3). In a similar study with adult patients, Kim et al. [22] found no statistically significant difference in cumulative effective dose between arterial and venous phases ($p = 0.186$) but significant difference between arterial and combined phases ($p < 0.001$). The non-significant difference found in the current study could be due to the use of trauma mattress, equipment design, and size-specific paediatric protocols which are known to affect CT doses [23–25]. Table 6 shows the estimated WBCT EDs for newborn and child phantoms. The result shows differences in ED between optimised arterial phase-only (9.1 A) protocol and combined arterial and venous phase (9.1B) protocols. The newborn phantom protocols resulted in lower EDs than the child phantom protocols. This indicates the need for radiographers to use appropriate protocols based on patients' age/size and clinical history. The WBCT EDs from this study are lower than Munk et al.'s [26] reported EDs for WBCTs of around 20.8 mSv. Low dose WBCT protocols has been

**Table 4** CT examination parameters for GE scanner protocols

| No. | Scan Mode | Noise Index | Auto-prescription | Pitch | Tube voltage [kVp] | Tube current [mAs] | $CTDI_{vol}$ [mGy] | DLP [mGy.cm] | ED [mSv] | SNR | FOM | IQ |
|---|---|---|---|---|---|---|---|---|---|---|---|---|
| Newborn Head Protocols | | | | | | | | | | | | |
| GBH | Axial | 18 | On | 1.00 | 100 | 162.53 | 13.96 | 167.58 | 1.40 | 3.83 | 10.48 | 2 |
| Newborn Arterial Phase CAP Protocols | | | | | | | | | | | | |
| GB1 | Axial | 18 | Off | 1.00 | 80 | 150 | 0.99 | 20.28 | 1.200 | 4.23 | 14.91 | 3 |
| GB2 | Axial | 28 | Off | 1.00 | 80 | 240 | 1.59 | 33.46 | 1.900 | 3.22 | 5.46 | 4 |
| GB3 | Helical | 18 | Off | 0.52 | 80 | 207 | 2.35 | 59.72 | 3.400 | 4.1 | 4.94 | 4 |
| GB4 | Helical | 20 | On | 0.52 | 80 | 122 | 2.32 | 40.79 | 2.900 | 5.2 | 9.32 | 4 |
| GB5 | Axial | 20 | Off | 1.00 | 80 | 200 | 1.33 | 27.85 | 1.600 | 3.43 | 7.35 | 3 |
| Newborn Arterial Phase CAP + Venous Phase AP Protocols | | | | | | | | | | | | |
| GBI | Axial | 18 | Off | 1.00 | 80 | 150.02 | 1.98 | 34.80 | 2.7 | 9.26 | 9.26 | 4 |
| GBII | Helical | 20 | Off | 0.98 | 100 | 247.52 | 3.45 | 92.16 | 5.8 | 1.18 | 1.18 | 3 |
| GBIII | Helical | 20 | Off | 0.98 | 80 | 250.02 | 1.86 | 49.62 | 3.2 | 2.97 | 2.97 | 3.5 |
| Child Head Protocols | | | | | | | | | | | | |
| GCH | Axial | 26 | On | 1.00 | 120 | 177.53 | 26.91 | 376.75 | 1.10 | 8.08 | 59.35 | 4 |
| Child Arterial Phase CAP Protocols | | | | | | | | | | | | |
| GC1 | Helical | 26 | On | 0.52 | 100 | 98.79 | 2.10 | 96.38 | 3.30 | 7.13 | 15.41 | 4 |
| GC2 | Helical | 20 | Off | 0.52 | 100 | 140.76 | 4.24 | 120.45 | 2.80 | 6.11 | 13.33 | 4 |
| GC3 | Axial | 20 | Off | 1.00 | 100 | 300.21 | 4.69 | 197.14 | 4.40 | 7.21 | 11.81 | 4 |
| Child Arterial Phase CAP + Venous Phase AP Protocols | | | | | | | | | | | | |
| GCI | Helical | 26 | On | 0.52 | 100 | 103.27 | 4.28 | 161.69 | 4.7 | 7.45 | 11.81 | 4 |
| GCII | Helical | 20 | Off | 0.98 | 100 | 143.01 | 2.36 | 104.99 | 3.2 | 5.52 | 9.52 | 3.5 |

**Key**: IQ = mean of the subjective image quality assessment for overall diagnosability on a scale of 1–5

**Table 5** CT examination parameters for Siemens scanner protocols

| No. | Scan Mode | Quality reference mAs | Pitch | Tube voltage [kVp] | Tube current [mA] | $CTDI_{vol}$ [mGy] | DLP [mGy.cm] | ED [mSv] | SNR | FOM | IQ |
|---|---|---|---|---|---|---|---|---|---|---|---|
| | | Newborn Head Protocol | | | | | | | | | |
| SBH | Helical | 300 | 0.600 | 100 | 91.0 | 13.24 | 280.05 | 1.20 | 2.67 | 5.94 | 3 |
| | | Newborn Trunk Protocols | | | | | | | | | |
| SB1 | Helical | 740 | 1.400 | 70 | 137.0 | 0.71 | 18.18 | 1.60 | 3.83 | 9.17 | 2 |
| SB2 | Helical | 740 | 1.400 | 80 | 129.0 | 0.67 | 16.53 | 1.50 | 4.54 | 13.74 | 3 |
| SBI | Helical | 740 | 1.400 | 80 | 117.00 | 0.92 | 19.76 | 1.80 | 5.14 | 14.68 | 3 |
| SBII | Helical | 576 | 1.400 | 70 | 147.00 | 0.93 | 14.91 | 1.70 | 3.91 | 8.99 | 2 |
| | | Child Head Protocol | | | | | | | | | |
| SCH | Helical | 461 | 0.600 | 100 | 169.0 | 24.58 | 386.14 | 1.00 | 7.58 | 57.46 | 4 |
| | | Child Trunk Examinations | | | | | | | | | |
| SC1 | Helical | 662 | 1.400 | 80 | 306.00 | 1.59 | 71.94 | 3.60 | 5.55 | 8.56 | 4 |
| SC2 | Helical | 662 | 1.400 | 70 | 294.00 | 1.52 | 72.37 | 3.50 | 5.23 | 7.82 | 3 |
| SCI | Helical | 488 | 1.100 | 70 | 440 | 2.13 | 81.45 | 4.42 | 4.2 | 3.99 | 3 |
| SCII | Helical | 318 | 1.400 | 80 | 447 | 2.08 | 79.80 | 4.30 | 5.15 | 6.17 | 2 |

**Key**: IQ = mean of the subjective image quality assessment for overall diagnosability on a scale of 1–5

shown to significantly reduce patient dose in comparison with standard protocols for all age groups [27].

### Image quality (SNR)

The Rose model [28, 29] stipulates that a signal should be five standard deviations from the above background to be detectable. This implies that diagnostic images with SNR > 5 are deemed to be of good quality. The SNRs of all tested child protocols were above 5, while some of newborn protocols had SNRs below 5. This may be due to the non-human equivalent CT numbers used in the newborn phantom.

Consistent with literature [22, 30], the study found no significant difference in IQ between examinations performed with arterial phase-only protocols and the combined arterial and venous phase protocols, although latter had higher estimated SNRs. However, the use of a combined arterial and venous phase increases the specificity of arterial injury detection [30], necessitating the use of this protocol in such clinical situations.

### Dose optimisation

Many dose optimisation strategies exist [13–15]. In this study, the FOM approach [16] was used in selecting the optimum protocols. All the selected protocols had FOMs above 5.0, indicating an increase in efficacy [16].

Consistent with report from the American Association of Physicists in Medicine (AAPM) [31], changes in the IQ reference parameters (noise index and quality reference mAs) affected the dose and image quality. Protocol GB3 with a lower noise index than protocol GB4 resulted in a higher mAs and lower $CTDI_{vol}$, although the relationship between the dose and image quality was affected by other parameters such as the pitch, slice thickness, and auto-prescription. The same trend was found for protocols GC1 and GC2.

It is recommended that different noise indexes should be used for different slice thickness due to differences in image noise relative to slice thickness [31]. In this study, the average slice thickness used for GE and siemens scanners were different, which could influence their respective dose and image quality. The thin-slice images may result in reduced image quality due to increased image noise, which may necessitate the use of higher radiation dose to obtain optimum image quality [32]. However, recent advancements in image reconstruction algorithms may help overcome this trade-off [33]. Nonetheless, a careful consideration of technique parameters should be made to enhance the efficiency of these protocols.

### Organ doses

The estimated organ doses for the brain were lower than the eye lens. This was consistent with previous studies in which the dose to the eye lenses was higher than the dose to the brain from both the DoseWatch and CT-Expo software [34] and from VirtualDose™ CT (VDCT) (Virtual phantoms Inc.,

**Table 6** Estimated WBCT ED

| Optimised protocol | GE scanner | | | Siemens scanner | | |
|---|---|---|---|---|---|---|
| | $ED_{WB}$ (mSv) | | Difference | $ED_{WB}$ (mSv) | | Difference |
| | 9.1 A | 9.1B | | 9.1 A | 9.1B | |
| Newborn | 2.6 | 4.1 | 57.69% | 2.7 | 3.0 | 11.11% |
| Child | 4.4 | 5.8 | 31.82% | 4.6 | 5.3 | 15.22% |

**Key**: $ED_{WB}$ = Whole-body CT effective dose; 9.1 A = dose from head + arterial phase CAP protocols; 9.1B = dose from head + arterial phase CAP + venous phase AP protocols

Albany, USA) for both age groups < 1 year and 6–10 years [35]. In general, the organ doses estimated from the 9.1B protocols were higher than the 9.1 A protocols. This could be due to overlap in scan areas from the multiphase 9.1B examinations. Nonetheless, the organ doses to the selected organs of the trunk from this study were lower than those estimated in the study by Gao et al. [35]. In that study, it was found that the dose to the male gonads for age group < 1 year to be 3.2 mSv against 2.10 mSv from this study and 9.9 and 8.5 mSv respectively for child examinations against 4.65 and 4.4 mSv to testis and ovaries respectively from this study. Similarly, this study's organ doses were within acceptable ranges and were lower than values indicated in literature [36, 37].

### Limitations

The study did not assess the influence of other parameters such as pitch, slice thickness, and scan length due to the fewer number of scans performed. The non-human equivalent CT numbers in the newborn phantom also limited the assessment of the image quality.

## Conclusion

The estimated $ED_{WB}$ from this study were lower than established values, although the study found higher doses for combined arterial and venous phase protocols due to the double sequence used. The use of appropriate image quality reference parameters (noise index and quality reference mAs) should be used by considering the slice thickness and patient body size when scanning with the GE Revolution CT and the Siemens SOMATOM Definition edge CT scanners at the study site. It is recommended that adequate assessment of patient's clinical history should be made when deciding on which protocol to use.

#### Abbreviations

| | |
|---|---|
| AAPM | American Association of Physicists in Medicine |
| CAP | Chest-abdomen-pelvic |
| CT | Computed tomography |
| CTDIvol | Volume computed tomography dose index |
| DLIR | Deep learning iterative reconstruction |
| DLP | Dose length product |
| ED | Effective dose |
| FAST | Focussed assessment with sonography for trauma |
| FOM | Figure-of-merit |
| GE | General Electric |
| IOR | Inter-observer reliability |
| IQ | Image quality |
| mSv | Milli-Sievert |
| NI | Noise index |
| ROI | Region of interest |
| SNR | Signal-to-noise ratio |
| VDCT | Virtual dose computed tomography |
| WBCT | Whole body computed tomography |
| WBCTED | Effective dose from whole body computed tomography |

## Supplementary Information

The online version contains supplementary material available at https://doi.org/10.1186/s12880-025-01675-4.

Supplementary Material 1

#### Acknowledgements

The authors acknowledge the Norwegian government NORPART project coordinators, both in Ghana and Norway, for the support offered to JLA. Particularly, the support provided by Pal Erik Goa to JLA during the latter's study period at NTNU is much appreciated.

#### Author contributions

JLA: Conceptualisation, methodology, investigation, project management, formal analysis, writing– original draft; SI: Conceptualisation, methodology, supervision, software, writing– review and editing; BOB: Conceptualisation, methodology, supervision, writing– review and editing; AL: Conceptualisation, investigation, resources, supervision; ISB: Conceptualisation, investigation, resources.

#### Funding

JLA received funding from the Norwegian government (NORPART Project) to undertake an eight-month master's exchange at the Norwegian University of Science and Technology. No other funding was received.

#### Data availability

The data associated with this will be made available by the corresponding author upon reasonable request.

### Declarations

#### Ethical approval

Not applicable.

#### Consent to participate

Not applicable.

#### Consent for publication

Not applicable.

#### Competing interests

The authors declare no competing interests.

#### Author details

[1]Department of Radiography, School of Biomedical and Allied Health Sciences, College of Health Sciences, University of Ghana, Korle-Bu Campus, Korle-Bu, P. O. Box KB 143, Accra, Ghana
[2]Department of Nuclear Safety and Security, School of Nuclear and Allied Sciences, College of Basic and Applied Sciences, University of Ghana, Atomic Campus, Accra, Ghana

[3]Department of Medical Physics, School of Nuclear and Allied Sciences, College of Basic and Applied Sciences, University of Ghana, Atomic Campus, Accra, Ghana
[4]Radiation Protection Institute (RPI), Ghana Atomic Energy Commission, Accra, Ghana
[5]Department of Midwifery and Radiography, School of Health & Psychological Sciences, University of London, London, UK
[6]Medical Physics Unit, Innlandet Hospital, Hamar, Norway

Received: 3 January 2025 / Accepted: 14 April 2025
Published online: 17 April 2025

**References**

1. Meulepas JM, Ronckers CM, Smets A, Nievelstein RAJ, Gradowska P, Lee C, Hauptmann M. Radiation exposure from pediatric CT scans and subsequent Cancer risk in the Netherlands. J Natl Cancer Inst. 2019;111(3):256–63. https://doi.org/10.1093/jnci/djy104.
2. Hemke R, Yang K, Husseini J, Bredella MA, Simeone FJ. Organ dose and total effective dose of whole-body CT in multiple myeloma patients. Skeletal Radiol. 2020;49(4):549–54. https://doi.org/10.1007/s00256-019-03292-z.
3. Kahn J, Grupp U, Kaul D, Boning G, Lindner T, Streitparth F. Computed tomography in trauma patients using iterative reconstruction: reducing radiation exposure without loss of image quality. Acta Radiol. 2016;57(3):362–9. https://doi.org/10.1177/0284185115580839.
4. Long B, April MD, Summers S, Koyfman A. Whole body CT versus selective radiological imaging strategy in trauma: an evidence-based clinical review. Am J Emerg Med. 2017;35(9):1356–62. https://doi.org/10.1016/j.ajem.2017.03.048.
5. Huber-Wagner S, Kanz KG, Hanschen M, van Griensven M, Biberthaler P, Lefering R. Whole-body computed tomography in severely injured patients. Curr Opin Crit Care. 2018;24(1):55–61. https://doi.org/10.1097/MCC.0000000000000474.
6. Arruzza E, Chau S. Whole-body CT. In: Hayre SC C, editor. Computed tomography: advanced clinical applications. 1st ed. Singapore: Springer; 2023. pp. 99–107.
7. Marsden NJ, Tuma F, Polytraumatized Patient. StartPearls Publishing; 2022 [Available from: https://www.ncbi.nlm.nih.gov/books/NBK554426/
8. Stengel D, Mutze S, Guthoff C, Weigeldt M, von Kottwitz K, Runge D, Kahl T. Association of Low-Dose Whole-Body computed tomography with missed injury diagnoses and radiation exposure in patients with blunt multiple trauma. JAMA Surg. 2020;155(3):224–32. https://doi.org/10.1001/jamasurg.2019.5468.
9. Jiang ZY, Wang HQ, Whole-Body CT, for Children After Trauma. Undefined efficacy with clear Cancer risks. Pediatr Crit Care Med. 2019;20(8):799. https://doi.org/10.1097/PCC.0000000000002003.
10. Gariani J, Martin SP, Botsikas D, Becker CD, Montet X. Evaluating the effect of increased pitch, iterative reconstruction and dual source CT on dose reduction and image quality. Br Jour Radiol. 2018;91. https://doi.org/10.1259/bjr.20170443.
11. International Atomic Energy Agency. Radiation protection and safety of radiation sources: international basic safety standards, IAEA safety standards series no. GSR part 3. Vienna: IAEA; 2014.
12. International Commission on Radiological Protection. The 2007 recommendations of the international commission on radiological protection publication 103. Ann ICRP 2007. 2007;37(2–4):326–30.
13. Almohiy H. Paediatric computed tomography radiation dose: A review of the global dilemma. World J Radiol. 2014;6(1):1–6. https://doi.org/10.4329/wjr.v6.i1.1.
14. Botwe BO, Schandorf C, Inkoom S, Faanu A. Variability of redundant scan coverages along the Z-axis and dose implications for common computed tomography examinations. J Med Imaging Radiat Sci. 2022;53(1):113–22. https://doi.org/10.1016/j.jmir.2021.10.007.
15. Kalra MK, Sodickson AD, Mayo-Smith WW. CT radiation: key concepts for gentle and wise use. Radiographics. 2015;35(6):1706–21. https://doi.org/10.1148/rg.2015150118.
16. Pace E, Borg M. Optimisation of a paediatric Ct brain protocol: A Figure-of-Merit approach. Radiat Prot Dosimetry. 2018;182(3):394–404. https://doi.org/10.1093/rpd/ncy078.
17. Ebdon-Jackson S, Frija G, European Society of R. Improving justification of medical exposures using ionising radiation: considerations and approaches from the European society of radiology. Insights Imaging. 2021;12(1):2. https://doi.org/10.1186/s13244-020-00940-0.
18. Rogers J, Revesz A. Experimental and quasi-experimental designs. The Routledge handbook of research methods in applied linguistics. 2019:133–43.
19. International Electrotechnical Commission (IEC). 61223-3-5. Evaluation and routine testing in medical imaging departments-part 3–5: Acceptance and constancy tests-image performance of computed tomography X-ray equipment. 2019.
20. McHugh ML. Interrater reliability: the kappa statistics. Biochemia Med. 2012;22(3):276–82.
21. Thiessen MEW. Application of focused assessment with sonography for trauma in the intensive care unit. Clin Chest Med. 2022;43(3):385–92. https://doi.org/10.1016/j.ccm.2022.05.004.
22. Kim SJ, Ahn SJ, Choi SJ, Park DH, Kim HS, Kim JH. Optimal CT protocol for the diagnosis of active bleeding in abdominal trauma patients. Am J Emerg Med. 2019;37(7):1331–5. https://doi.org/10.1016/j.ajem.2018.10.011.
23. Karappara J, Koteshwar P, Panakkal NC, Sukumar S. Optimization of pediatric CT brain protocol to achieve reduced patient dose. Biomedical Pharmacol J. 2020;13(1):391–7. https://doi.org/10.13005/bpj/1899.
24. Kamdem FE, Ngano SO, Alla Takam C, Fotue AJ, Abogo S, Fai CL. Optimization of pediatric CT scans in a developing country. BMC Pediatr. 2021;21(1):44. https://doi.org/10.1186/s12887-021-02498-2.
25. Hemmes B, Jeukens CR, Kemerink GJ, Brink PR, Poeze M. Effect of spinal immobilisation devices on radiation exposure in conventional radiography and computed tomography. Emerg Radiol. 2016;23(2):147–53. https://doi.org/10.1007/s10140-015-1371-0.
26. Munk RD, Strohm PC, Saueressig U, Zwingmann J, Uhl M, Südkamp NP, Bley TA. Effective dose Estimation in whole-body multislice CT in paediatric trauma patients pediatric radiology. 2009;39(3):245–52 https://doi.org/10.1007/s00247-008-1091-7
27. Simma L, Fornaro J, Stahr N, Lehner M, Roos JE, Lima TVM. Optimising whole body computed tomography doses for paediatric trauma patients: a Swiss retrospective analysis. J Radiol Prot. 2022;42(2). https://doi.org/10.1088/1361-6498/ac6274.
28. Burgess AE. The Rose model, revisited. Journal of the optical society of America A, optics, image science, and vision. 1999;16(3):633–46 https://doi.org/10.1364/josaa.16.000633
29. Hsieh SS, Leng S, Yu L, Huber NR, McCollough CH. A minimum SNR criterion for computed tomography object detection in the projection domain medical physics. 2022;49(8):4988–98 https://doi.org/10.1002/mp.15832
30. Godt JC, Johansen CK, Martinsen ACT, Schulz A, Brogger HM, Jensen K, Dormagen JB. Iterative reconstruction improves image quality and reduces radiation dose in trauma protocols; A human cadaver study. Acta Radiol Open. 2021;10(10):20584601211055389. https://doi.org/10.1177/20584601211055389.
31. American Association of Physicists in Medicine. AAPM Computed Tomography Radiation Dode Education Slides. 2013.
32. Riedel CH, Zoubie J, Ulmer S, Gierthmuehlen J, Jansen O. Thin-slice reconstructions of nonenhanced CT images allow for detection of thrombus in acute stroke. Stroke. 2012;43(9):2319–23. https://doi.org/10.1161/STROKEAHA.112.649921.
33. Schaller F, Sedlmair M, Raupach R, Uder M, Lell M. Noise reduction in abdominal computed tomography applying iterative reconstruction (ADMIRE). Acad Radiol. 2016;23(10):1230–8. https://doi.org/10.1016/j.acra.2016.05.016.
34. Akyea-Larbi KO, Hasford F, Inkoom S, Tetteh MA. Patient dose Estimation in CT examination using dose conversion coefficient method and CT -expo software. Health Technol. 2022;12(4):809–14. https://doi.org/10.1007/s12553-022-00683-6.
35. Gao Y, Quinn B, Pandit-Taskar N, Behr G, Mahmood U, Long D, Dauer LT. Patient-specific organ and effective dose estimates in pediatric oncology computed tomography. Phys Med. 2018;45:146–55. https://doi.org/10.1016/j.ejmp.2017.12.013.
36. Yu L, Liu X, Leng S, Kofler JM, Ramirez-Giraldo JC, Qu M, McCollough CH. Radiation dose reduction in computed tomography: techniques and future perspective. Imaging Med. 2009;1(1):65–84. https://doi.org/10.2217/iim.09.5.
37. Akyea-Larbi KO, Tetteh MA, Martinsen ACT, Hasford F, Inkoom S, Jensen K. Benchmarking of a new automatic Ct radiation dose calculator. Radiat Prot Dosimetry. 2020;191(3):361–8. https://doi.org/10.1093/rpd/ncaa167.

## Publisher's note